Electronic Supplementary Material (ESI) for Journal of Materials Chemistry C.

Supplementary Information for

Pressure-induced emission enhancement in hexaphenylsilole: a computational study

Tian Zhang,[ab] Wen Shi,[b] Dong Wang,[b] Shuping Zhuo,[a] Qian Peng*[c] and Zhigang Shuai*[b]

[a] School of Chemistry and Chemical Engineering, Shandong University of Technology, Zibo 255049, P. R. China.

[b] MOE Key Laboratory of Organic OptoElectronics and Molecular Engineering, Department of Chemistry, Tsinghua University, Beijing 100084, P. R. China. *E-mail: zgshuai@tsinghua.edu.cn

[c] CAS Key Laboratory of Organic Solids, Institute of Chemistry, Chinese Academy of Sciences, Beijing 100190, P. R. China. *E-mail: qpeng@iccas.ac.cn

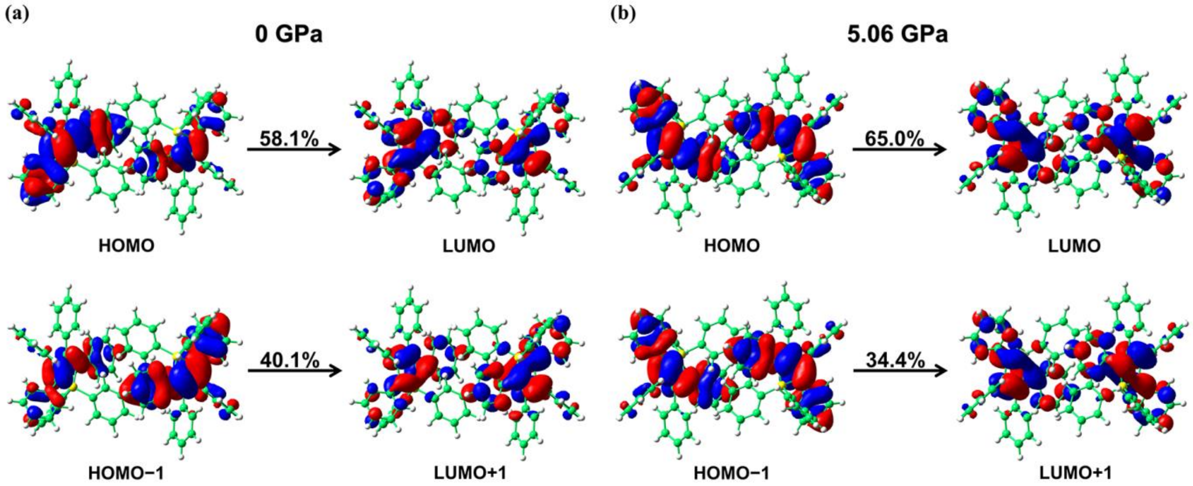

Fig. S1 Electron density contours of the transition orbitals and the transition proportions of the S_1 states for the dimers with maximum *J* at 0 GPa (a) and 5.06 GPa (b).

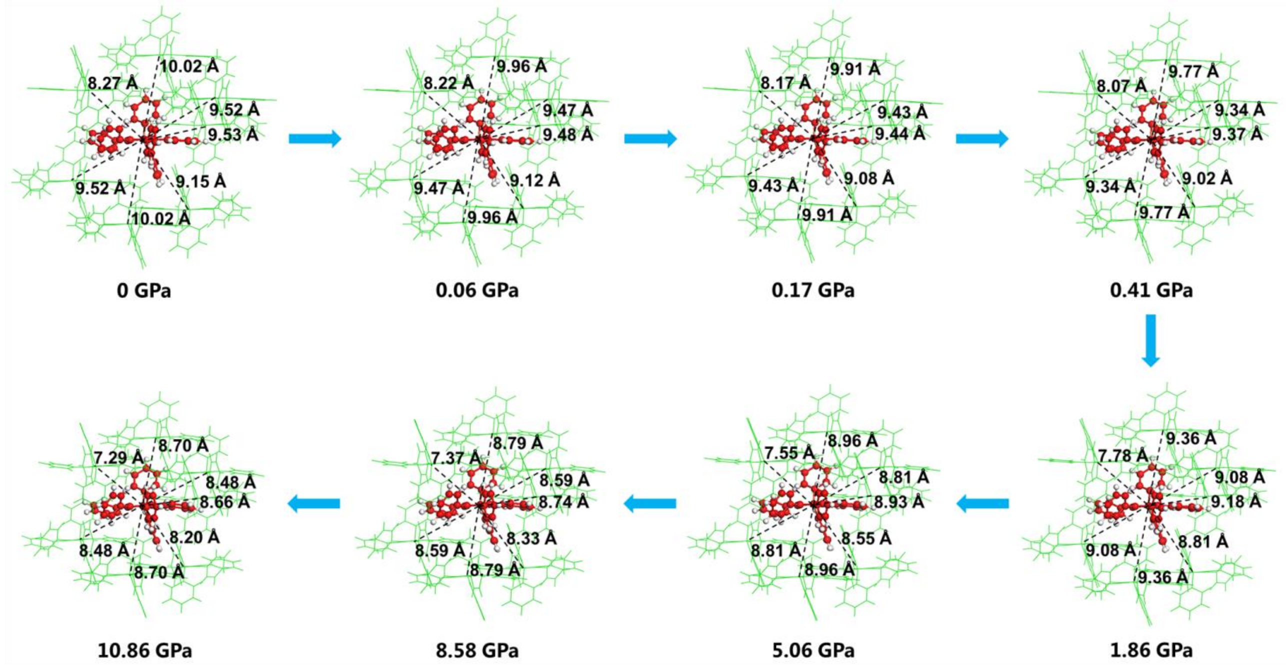

Fig. S2 Evolution of the molecular packing structure of HPS aggregates within ~10 Å of the QM centroid with the compression stress.

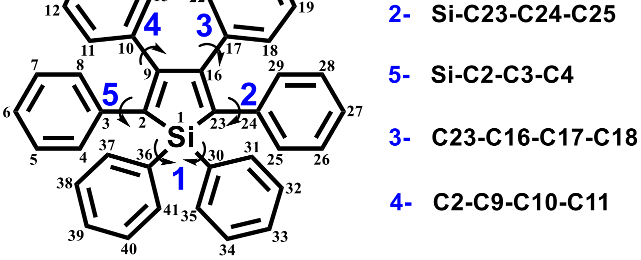

Fig. S3 Molecular structure of HPS with the labeled atom index. Representative torsional angles at 2,3,4,5-positions are detailed in the right panel.

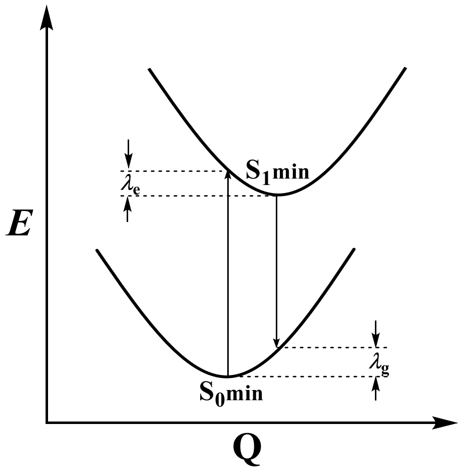

Fig. S4 Schematic representation of $\lambda_{g(e)}$ in the ground-state (excited-state) PES. Q refers to the nuclear configuration. **S_{0min}** and **S_{1min}** represent the most stable optimized structures in the S_0 and S_1 states.

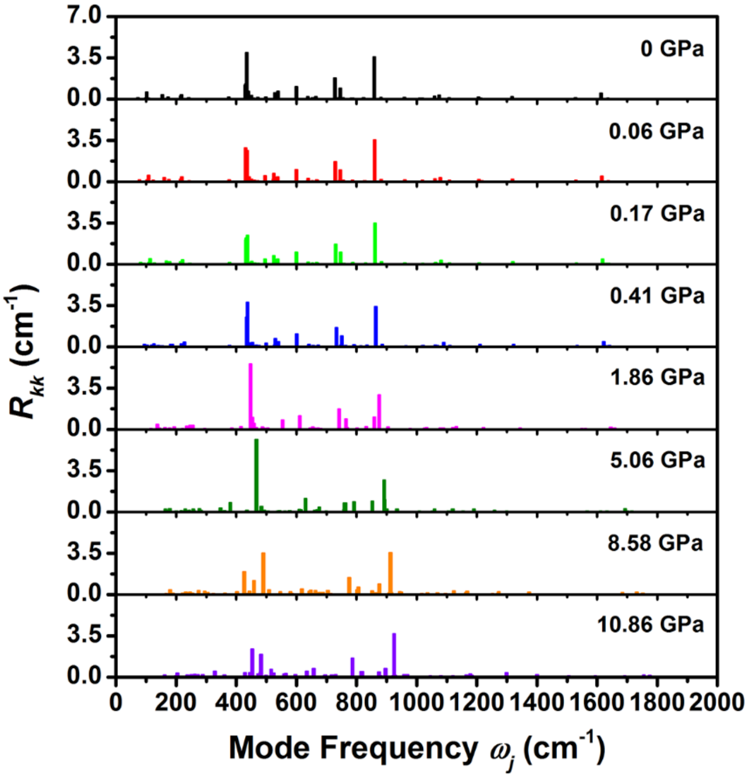

Fig. S5 Diagonal elements R_{kk} of the electronic R_{kl} versus mode frequency ω_j for HPS in aggregates at different pressures.

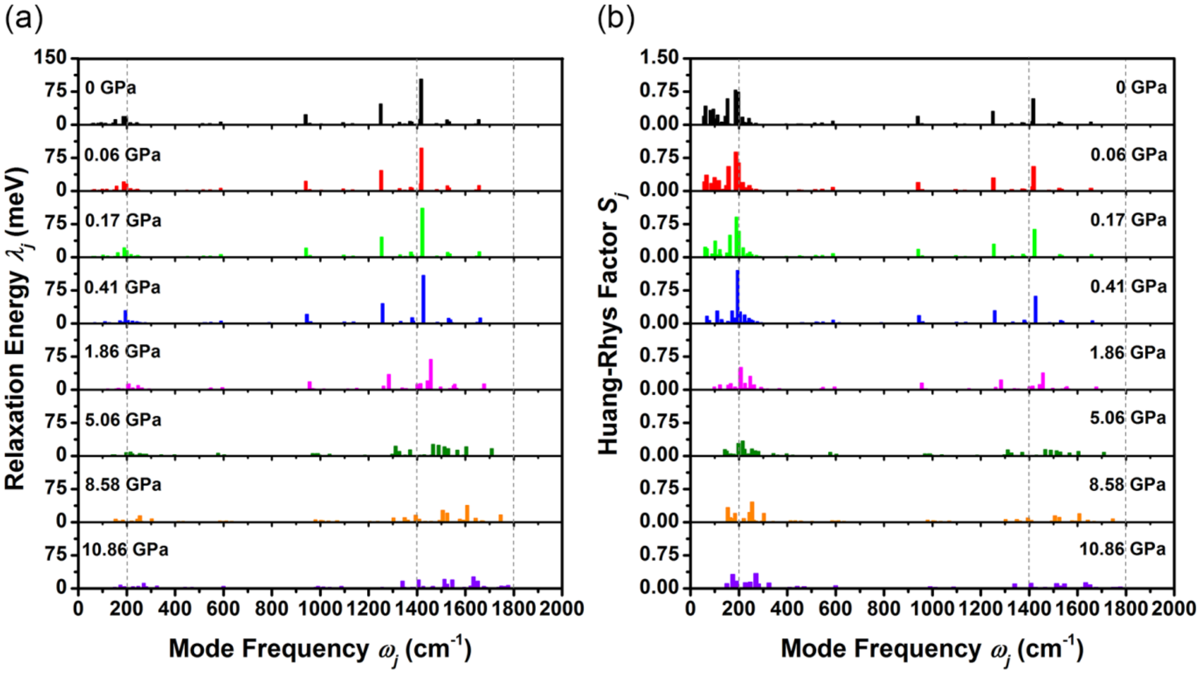

Fig. S6 Relaxation energy λ_j (a) and Huang-Rhys factor S_j (b) of each normal mode versus mode frequency ω_j of HPS in aggregates at different pressures in the excited-state PES.

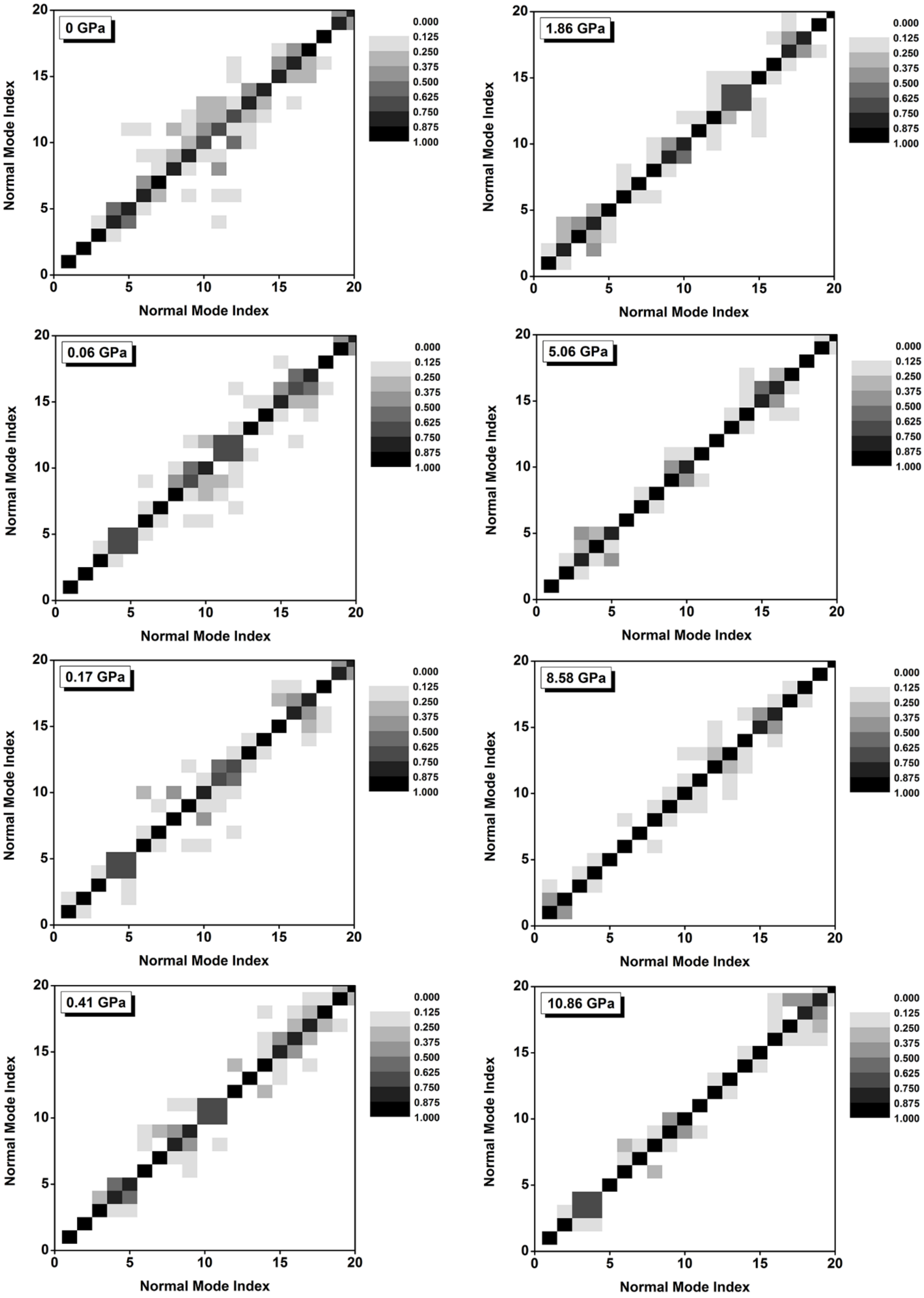

Fig. S7 Contour maps of the DRM for the lowest 20 modes of HPS in aggregates at different pressures. The excited-state normal mode index is rearranged to make the largest element the diagonal.

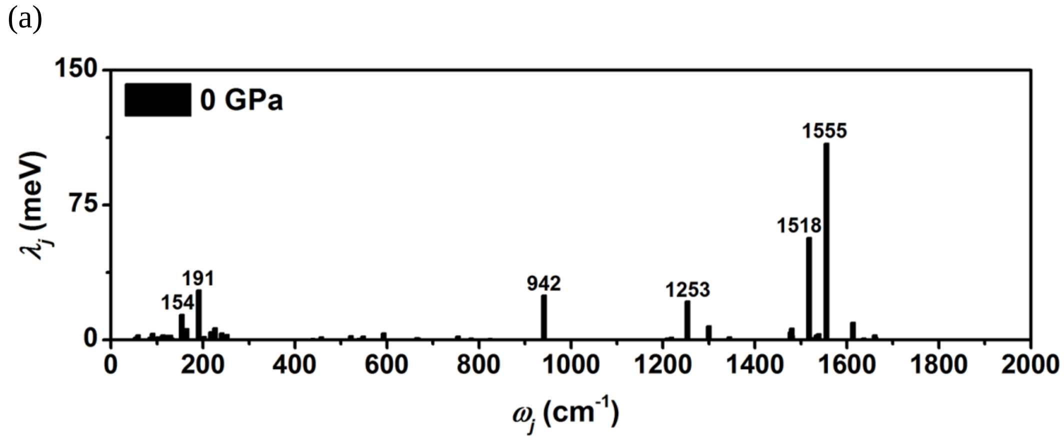

(b)

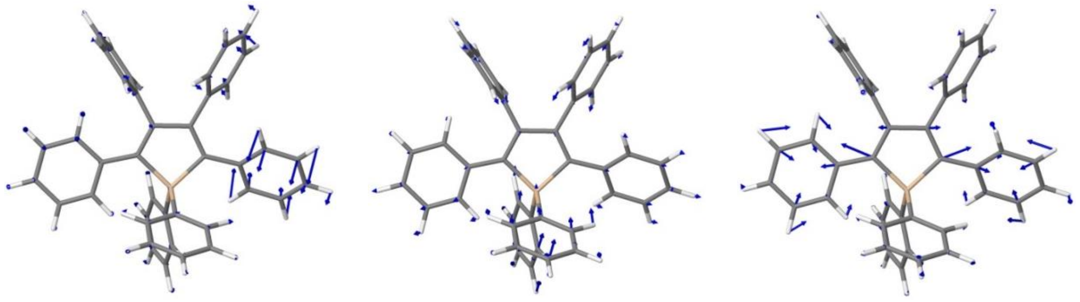

Mode 16, 154 cm^{-1} Mode 19, 191 cm^{-1} Mode 83, 942 cm^{-1}

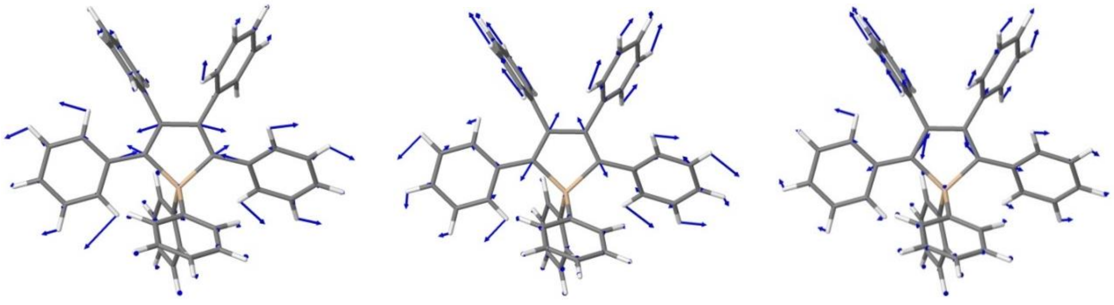

Mode 137, 1253 cm^{-1} Mode 158, 1518 cm^{-1} Mode 164, 1555 cm^{-1}

Fig. S8 Calculated λ_j versus ω_j (a) and diagrammatic illustration of selected normal modes with large λ_j (b) of HPS in aggregates at ambient pressure (0 GPa).

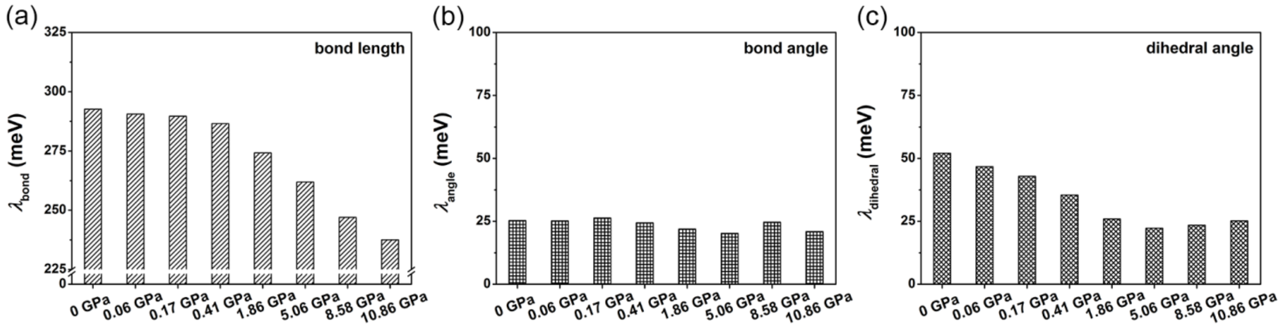

Fig. S9 Projection of the total relaxation energy λ_e onto the internal coordinates of HPS in aggregates at different pressures, including λ_{bond} (a), λ_{angle} (b) and $\lambda_{dihedral}$ (c).

Table S1 Comparison of the lattice constants (*a*, *b*, *c*, *α*, *β*, *γ*), volume (*V*) and density (*ρ*) of the unit cell of the naphthalene crystal at different pressures obtained from the experimental measurements (*exp*.) and DFT-D calculations (*cal*.).

Pressure (GPa)	*a* (Å)	*b* (Å)	*c* (Å)	*α* (°)	*β* (°)	*γ* (°)	*V* (Å^3)	*ρ* (g·cm^{-3})
				exp.				
0	8.235	6.003	8.658	90	122.92	90	359.28	1.185
0.4	8.035	5.890	8.565	90	123.59	90	337.65	1.261
0.6	7.995	5.873	8.542	90	123.68	90	333.74	1.275
1.0	7.852	5.811	8.474	90	124.03	90	320.44	1.328
2.1	7.678	5.721	8.395	90	124.55	90	303.71	1.402
				cal.				
0	8.179	6.026	8.787	90	123.93	90	359.28	1.185
0.4	7.598	5.698	8.303	90	124.15	90	297.46	1.431
0.6	7.556	5.675	8.282	90	124.22	90	293.68	1.449
1.0	7.486	5.637	8.246	90	124.39	90	287.13	1.483
2.1	7.377	5.579	8.189	90	124.72	90	277.04	1.537

Table S2 Lattice constants (*a*, *b*, *c*, *α*, *β*, *γ*), volume (*V*) and density (*ρ*) of the unit cell of the HPS crystal under different pressure values obtained from DFT-D calculations. The experimental (*exp*.) data at ambient pressure (0 GPa) are also given.

Pressure (GPa)	*a* (Å)	*b* (Å)	*c* (Å)	*α* (°)	*β* (°)	*γ* (°)	*V* (Å^3)	*ρ* (g·cm^{-3})
exp. 0	9.527	10.043	16.308	77.150	79.580	71.981	1436.05	1.246
0	9.523	10.021	16.332	76.948	79.638	72.317	1436.05	1.246
0.06	9.472	9.964	16.270	76.857	79.587	72.362	1414.61	1.265
0.17	9.430	9.906	16.187	76.912	79.609	72.383	1393.40	1.284
0.41	9.341	9.777	16.070	76.770	79.363	72.469	1351.60	1.324
1.86	9.079	9.361	15.730	76.226	79.051	72.992	1231.23	1.453
5.06	8.808	8.959	15.358	75.933	78.726	73.821	1118.23	1.600
8.58	8.592	8.785	15.040	75.294	78.270	74.528	1046.88	1.709
10.86	8.479	8.702	14.892	74.853	78.211	74.765	1012.37	1.767

Table S3 Calculated adiabatic excitation energies (ΔE), electric transition dipole moments (μ), oscillator strengths (f) and HOMO (H) → LUMO (L) assignments of S_1 for HPS in aggregates at different pressures.

Pressure (GPa)	ΔE (eV)	μ (D)	f	H→L
0	2.71	5.90	0.31	98.3%
0.06	2.70	5.92	0.31	98.3%
0.17	2.70	5.92	0.31	98.3%
0.41	2.69	5.94	0.31	98.3%
1.86	2.67	5.88	0.31	98.3%
5.06	2.66	5.76	0.30	98.2%
8.58	2.65	5.80	0.30	98.1%
10.86	2.65	5.83	0.30	98.0%

Table S4 Intermolecular distances for the dimer with maximum excitonic coupling (J) in HPS aggregates at different pressures. Relaxation energies in the ground-state (λ_g) and excited-state (λ_e) PES, as well as the ratios of J to $\lambda_{g(e)}$ ($J/\lambda_{g(e)}$).

Pressure (GPa)	Distance (Å)	J (meV)	λ_g (meV)	λ_e (meV)	J/λ_g	J/λ_e
0	9.15	16.02	380.98	370.03	0.042	0.043
0.06	9.12	16.28	374.64	362.46	0.043	0.045
0.17	9.08	16.48	370.46	358.92	0.044	0.046
0.41	9.02	17.05	359.47	346.43	0.047	0.049
1.86	8.81	18.27	336.95	322.14	0.054	0.057
5.06	8.55	19.49	318.30	304.47	0.061	0.064
8.58	8.33	20.74	308.93	295.07	0.067	0.070
10.86	8.20	21.49	298.66	283.67	0.072	0.076

Table S5 Intermolecular distances and excitonic couplings (J) for dimers in Fig. 2 at ambient pressure (0 GPa).

Distance (Å)	J (meV)
8.27	8.63
9.15	**16.02**
9.52	11.73
9.53	12.77
10.02	9.12

Table S6 Energy levels of HOMO, LUMO and the corresponding energy gaps ($\Delta E_{\text{H-L}}$) of HPS in aggregates at different pressures.

Pressure (GPa)	HOMO (eV)	LUMO (eV)	$\Delta E_{\text{H-L}}$ (eV)
0	−5.08	−1.60	3.48
0.06	−5.06	−1.59	3.47
0.17	−5.04	−1.58	3.46
0.41	−5.01	−1.57	3.44
1.86	−4.90	−1.50	3.40
5.06	−4.78	−1.42	3.36
8.58	−4.66	−1.35	3.31
10.86	−4.60	−1.32	3.28

Table S7 Relaxation energies of low-frequency modes (λ_{LF}) and high-frequency modes (λ_{HF}), as well as their contributions to the total λ_{e} for HPS in aggregates at different pressures.

Pressure (GPa)	λ_{LF} (meV)	λ_{HF} (meV)	λ_{e} (meV)	λ_{LF} / λ_{e}	λ_{HF} / λ_{e}
0	70	154	370	0.19	0.42
0.06	65	152	362	0.18	0.42
0.17	62	152	359	0.17	0.42
0.41	54	149	346	0.16	0.43
1.86	22	150	322	0.07	0.46
5.06	13	151	304	0.04	0.50
8.58	14	146	295	0.05	0.50
10.86	14	139	284	0.05	0.49

Table S8 Selected normal modes *j* with corresponding frequencies (ω_j), Huang-Rhys factors (S_j), relaxation energies (λ_j) and vibration types for HPS in aggregates at ambient pressure (0 GPa).

mode *j*	ω_j (cm^{-1})	S_j	λ_j (meV)	Vibration types^a
16	154	0.73	14.00	i (2-ring twisting), i (3,5-rings twisting)
19	191	1.17	27.64	i (1,1-rings deformation), iii (CSiC, CCSi)
83	942	0.21	24.91	iii (CCSi, 2,5-rings CCC), iv (2,5-rings), v (silole CC and CSi)
137	1253	0.14	21.55	iii (2,5-rings CCC), iv (2,3,4,5-rings), v (silole CC and CSi)
158	1518	0.30	56.93	iii (CSiC and 2,3,4,5-rings CCC), iv (2,3,4,5-rings), v (silole CC)
164	1555	0.57	109.31	iii (silole and 2,3,4,5-rings CCC), iv (2,3,4,5-rings), v (silole CC)

^{a}Vibration types: (**i**) benzene (heterocyclic) ring out-of-plane deformation/twisting vibration; (**ii**) CH out-of-plane rocking vibration; (**iii**) CCC (CSiC, CCSi) in-plane bending vibration; (**iv**) CH in-plane bending vibration; (**v**) CC (CSi) stretching vibration. The major contributed vibration type of each mode is underlined.

Table S9 Relaxation energies from bond length (λ_{bond}), bond angle (λ_{angle}), dihedral angle ($\lambda_{\mathrm{dihedral}}$) and the total ($\lambda_{\mathrm{g(e)}} = \lambda_{\mathrm{bond}} + \lambda_{\mathrm{angle}} + \lambda_{\mathrm{dihedral}}$) for HPS in aggregates at different pressures.

Pressure (GPa)	λ_{bond} (meV)	λ_{angle} (meV)	$\lambda_{\mathrm{dihedral}}$ (meV)	λ_{g} (meV)
0	303.15	30.35	47.48	380.98
0.06	302.67	30.33	41.64	374.64
0.17	301.34	30.72	38.40	370.46
0.41	298.90	30.54	30.03	359.47
1.86	286.93	28.38	21.64	336.95
5.06	271.94	28.78	17.58	318.30
8.58	254.81	33.99	20.13	308.93
10.86	243.56	32.56	22.54	298.66
Pressure (GPa)	λ_{bond} (meV)	λ_{angle} (meV)	$\lambda_{\mathrm{dihedral}}$ (meV)	λ_{e} (meV)
0	292.68	25.30	52.05	370.03
0.06	290.56	25.17	46.73	362.46
0.17	289.68	26.34	42.90	358.92
0.41	286.57	24.41	35.45	346.43
1.86	274.27	21.94	25.93	322.14
5.06	261.90	20.26	22.31	304.47
8.58	246.98	24.67	23.42	295.07
10.86	237.55	20.96	25.16	283.67